Joint EUROGRAPHICS - IEEE TCVG Symposium on Visualization (2003)
G.-P. Bonneau, S. Hahmann, C. D. Hansen (Editors)

Case Study: Comparing Two Methods for Filtering External Motion in 4D Confocal Microscopy Data

Wim de Leeuw and Robert van Liere

Center for Mathematics and Computer Science CWI, Amsterdam, Netherlands

Abstract

In this case study, we compare two methods for filtering external motion in time dependent volume data sets acquired from confocal microscopy. The pros and cons of a landmark based and a voxel based method are discussed. We show that filtering external motion is an essential first step for the visualization of confocal data.

Categories and Subject Descriptors (according to ACM CCS): I.3.3 [Computer Graphics]: Picture/Image Generation I.3.6 [Computer Graphics]: Methodology and Techniques
Keywords: volume visualization. registration, matching, biomedical imaging.

1. Introduction

In this case study, we compare two methods for filtering external motion in time dependent volume data sets. A time series was made of the process of decondensation of the chromatin after cell division (mitosis). During mitosis chromatin is densely packed in chromosomes. After mitosis, the chromatin decondensates to form a new nucleus. The aim of these experiments is to analyze the movement of chromatin. We classify the movement of chromatin as *internal movements* to the cell.

To acquire such time series, living cells are prepared and mounted on a slide which is placed under the confocal microscope. The time needed to acquire the time series data varies greatly, but usually is in the order of a few hours. Several problems occur during this time period that effect the data. Firstly, a cell can translate and rotate on the slide due to the forces exerted by neighboring cells. These movements are independent of the internal movements made by the chromatin during decondensation. Secondly, since the confocal microscope resides in a laboratory, vibrations caused by outdoor traffic, people walking, etc, will cause extra movements in the data. We classify both these movements as *external movements*.

The goal is to filter external movements, resulting in data that contain only the internal movement of the cell. Consider figure 1 which shows a snapshot from the time series of 3D data sets of the process of decondensation. The left image shows the results of a feature tracking algorithm applied to the raw data; i.e. internal and external movements. Feature tracks are drawn as lines in different colors. A gray scale slice of the final time step is superimposed in the image. The right image shows the feature tracks when applied to the data set after filtering the external movements; i.e. the tracks represent only internal movements †.

External motion filtering can be viewed as a rigid registration problem. The term registration as used in medical imaging means bringing into spatial alignment separately acquired images of the same object. When accurately registered, each separate image will have the same coordinate system and a given voxel in one image will represent the same physical volume as the corresponding voxel in another image. In general, all registration approaches have four steps in common: (1) define and extract a structure (as a point, surface or directly as a voxel), (2) linking of corresponding structures, (3) calculation of transformation parameters, (4) performing the transformation. Calculation of the transformation parameters is the most challenging part of the process. It may involve optimization of a prescribed cost function achieved by iterating on the solution. There

† The submitted MPEG videos show animations of the raw and filtered time series.

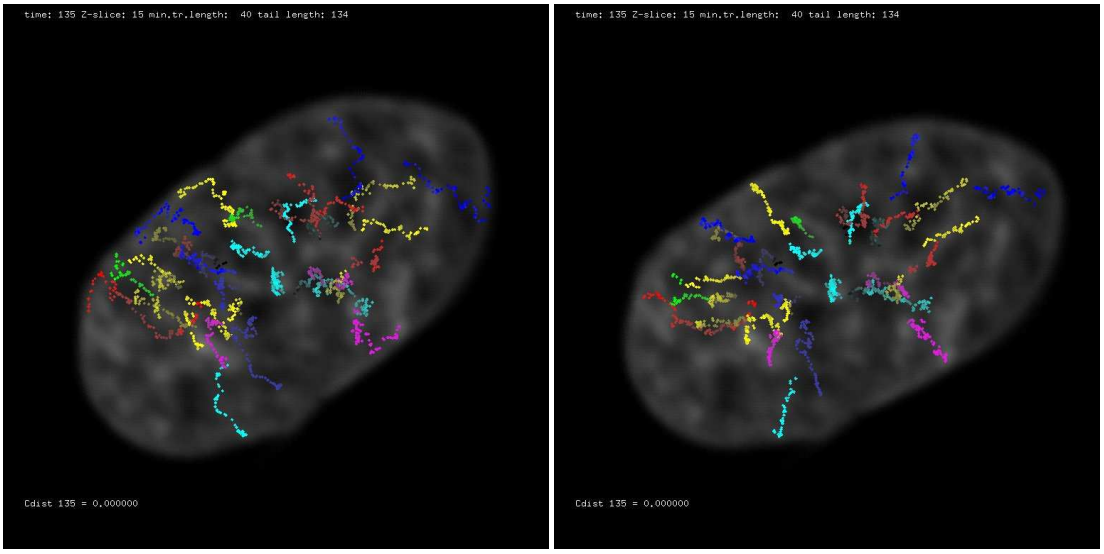

Figure 1: *Feature tracking applied to confocal data. The left image shows tracks of the raw data (internal and external motion). The right image shows tracks of the filtered data (internal motion only).*

are both rigid body and elastic types of transformations. In rigid body transformation, all the points and objects in an image are assumed to rotate/translate as a whole and do not rotate/translate relative to each other.

2. Related work

Image registration is a fundamental problem in medical imaging, resulting in the publication of hundreds of papers. Maintz and Viergever have recently published a comprehensive survey[1]. This survey classifies image registration techniques according to nine criteria: the dimensionality of the data, nature of the registration basis, nature of the transformation, domain of the transformation, interaction, optimization procedure, modalities involved, subject, and object.

Although the chromatin data set is not medical, we use these criteria to classify our approach. In particular, the nature of the registration basis of the two methods we have used are intrinsic based on landmarks and voxel properties. The nature of the transformation are global rigid transformations with six degrees of freedom; three translations and three rotations.

3. Method

3.1. Problem formulation

Assume two scalar data sets, M_a and M_b. A rigid transformation Φ is a function:

$$\hat{M}_b = \Phi(M_a, R, T) \tag{1}$$

in which every voxel in M_a is transformed to a corresponding voxel in $\hat{M}_b$. The transformation is a rotation R or a translation T. In addition, assume that a monotonic increasing comparison function $D()$ exists which quantifies the difference between two data sets; e.g. $D(M_a, M_b) = 0$ if there is no measurable difference between data sets M_a and M_b and $D(M_a, M_b) > D(M_c, M_d)$ if the difference between sets M_a and M_b is less than between M_c and M_d.

The rigid registration problem can now be formulated as:

$$\textit{minimize}\ \ D\,(M_b,\ \hat{M}_b); \tag{2}$$

subject to the free variables R and T; i.e. determine R and T such that the difference between the measured data M_b and the computed data $\hat{M}_b$ is minimized.

It is possible to solve this problem using, for example, Marquardt based fitting methods[2].

3.2. Method 1: Landmark Based Registration

In a previous paper we published a method to extract and track features in confocal data [3]. Feature positions are used as landmarks at each time step in the data sets. Since the feature tracking algorithm has computed the correspondence of features between two successive time steps, we may assume that a landmark a time t is in correspondence with a landmark at time $t+1$.

Denote the set of found landmark positions at time t as $M_t = \{m_t^1, \ldots m_t^N\}$ and define $\hat{M}_t = \Phi(M_t, R_t, T_t)$ as the set of landmarks which are found from applying the transformation Φ to all landmark positions in data set M_t. The landmark

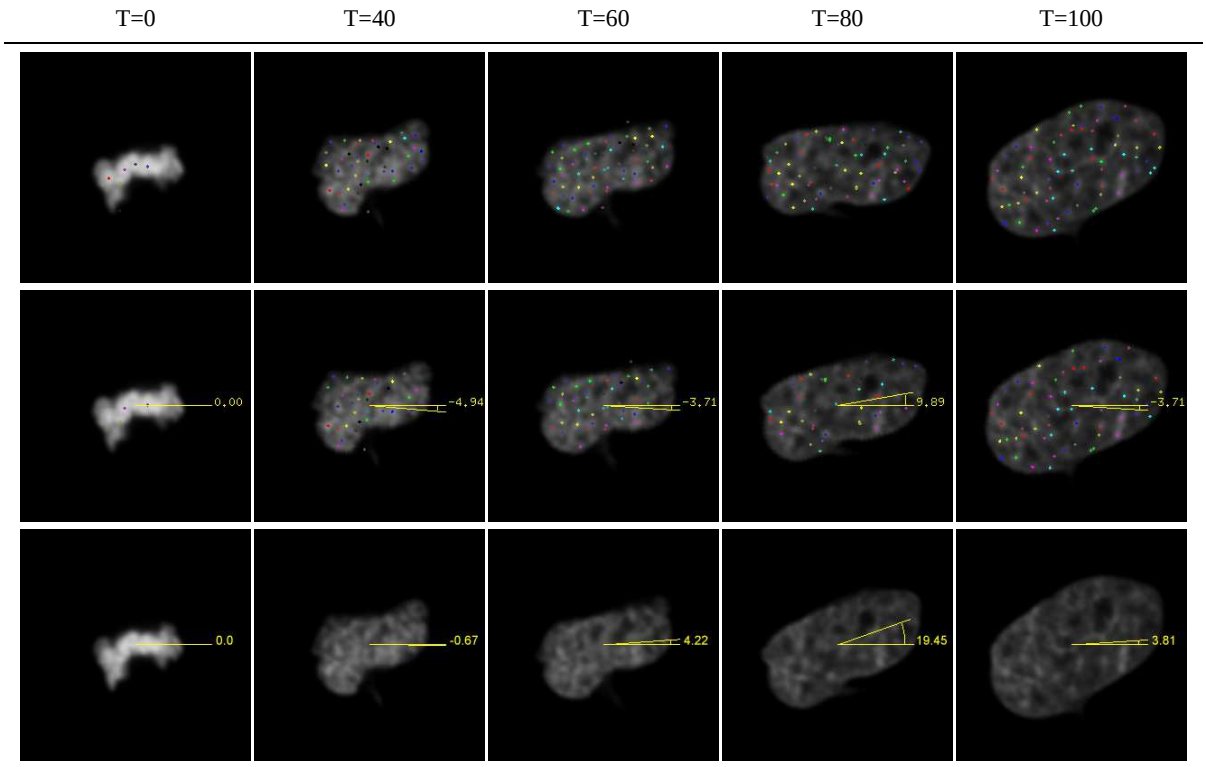

Figure 2: *The rotation angle in the XY-plane of the data in five time steps of the time series. The top row shows slices of raw data set and the found landmarks at each time step, The middle row shows slices using the landmark registration method. The yellow angle shows the rigid rotation with respect to the raw data. The bottom row shows the rotation angles found using the voxel based method.*

registration problem is now defined as to

$$minimize \;\; D\left(M_t, \hat{M}_{t-1}\right) \tag{3}$$

in which $D()$ is the sum of the distances between corresponding landmark positions;

$$D(M_t, \hat{M}_{t-1}) \;=\; \sum_{1}^{N} |m_t^i - \hat{m}_{t-1}^i| \tag{4}$$

3.3. Method 2: Voxel Based Registration

Assume a sequence of time dependent scalar data sets describing the movement of a mass distribution $M_0, M_1, \ldots M_N$. Define $\hat{M}_t \;=\; \Phi(M_t, R_t, T_t)$ as the computed mass distribution by applying the transformation Φ to each voxel in M_t.

The computation of R_t ad T_t is now formulated as an optimization problem:

$$minimize \;\; D\left(M_t, \hat{M}_{t-1}\right) \tag{5}$$

in which $D()$ is the sum of he absolute differences between corresponding voxels; i.e.

$$D(M_t, \hat{M}_{t-1}) \;=\; \sum_{i \in voxels} |M_t(i) \;-\; \hat{M}_{t-1}(i)| \tag{6}$$

4. Results

Visualization. The two registration methods were applied to a time series of the process of decondensation of chromatin after cell division (mitosis). The data set consists of a series of 134 3D data sets. Each data set consists of a stack of 32 optical sections of 256 $\times$ 256 pixels. Due to physical characteristics of a confocal microscope the resolution along the Z-direction is four times less than in the XY-plane. Registration was performed on all of the 134 3D data sets. For each time step t, M_{t+1} was registered with M_t resulting in 133 registration steps.

In this section we present only the results of rotations in the XY-plane. Similar results can be obtained from rotations in the YZ and XZ-planes. However, since the specimen mounted on the slide consists of only one layer of cells, it can be assumed that rotations in the XZ and YZ-planes are negligible. Both registration methods obtain in very small

translations. The magnitude of the largest found translation was well below the size of two voxels. Therefore, we disregard the found translations from our analysis.

Landmarks are detected using the Largest Contour Segmentation method [4]. This method selects landmarks based on local maxima in combination with additional criteria to discriminate significant extrema from noise. The correspondence of landmarks between time steps was established using an in-house developed multidimensional feature tracking algorithm [3].

Figure 2 shows the rotation angle in the XY-plane of the data in five time steps of the time series. The top row shows a 2D slice of raw data set. Landmark positions found in the 3D data are projected onto each slice. The middle row shows the same slices after registration using the landmark method. The rotation angle (drawn in yellow) shows the rigid rotation in the XY-plane of the data with respect to the raw data. The center of rotation is chosen as the center of the image. The bottom row shows the rotation angles found using the voxel based method.

Time steps $T = 60$, $T = 100$ and $T = 120$ in the row of raw images clearly show the rotations of the cell nucleus. The images in column $T = 100$ clearly show that the data has been filtered.

The top plot figure 3 graphs the computed rotation angle between time steps for both methods. Rotation angles for the landmark method are drawn in green, while angles for the voxel method are drawn in red. The largest found angle for a single timestep was for both methods just higher than 2 degrees (see angles at timestep 104).

The middle plot graphs the distribution of angle values. Seventeen bins with a size of 0.25 degrees were used to place the angle values. The plot indicates that the distribution is normal with a mean at 0 degrees.

The bottom plot graphs the difference of rotation angle for both methods; $diff_i = |M_1^{ang_i} - M_2^{ang_i}|$. The average difference between the found angle is 0.31 degrees. The average angle difference for the first 40 time steps is 0.63, while the average angle difference from time step 40 till the end of the series is 0.17.

The plot in figure 4 graphs the accumulated rotation angle for both methods; $accum_n = \sum_1^n ang_i$. The accumulated rotations occurring between $T = 60$ and $T = 100$ show a systematic rotation in one direction for a long period. Such a systematic rotation is not immediately obvious from the plots in figure 3.

The shape of the two graphs in figure 4 are very similar, from time step 40 till the end of the time series

Cell Biology. Filtering external motion is the first step for further analysis and visualization of the data. As can be seen in figure1 external motion clearly influences the feature tracking algorithm.

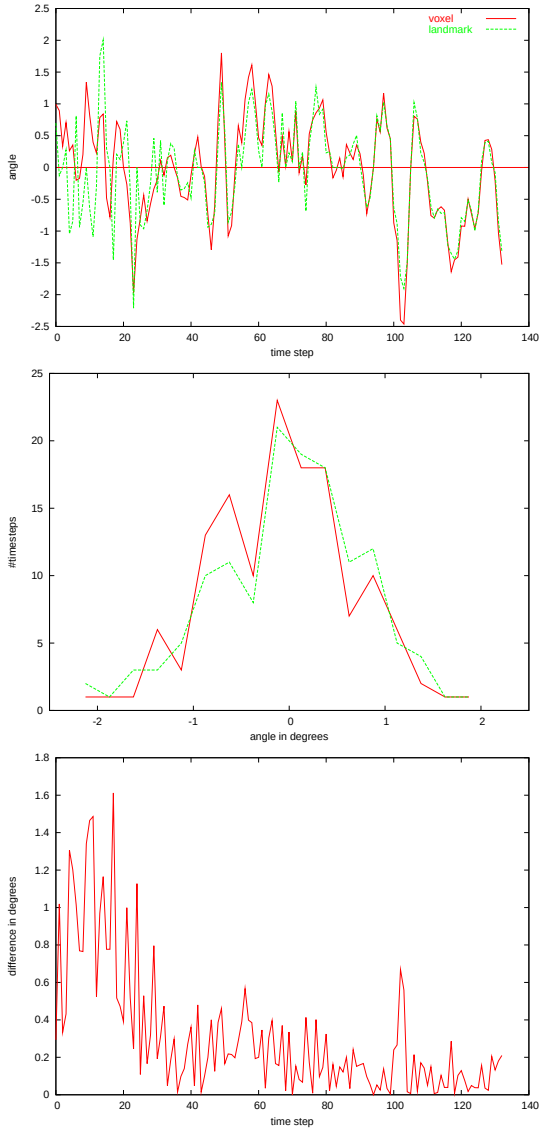

Figure 3: *Angles found by the registration algorithms. The top plot shows the found angles for the landmark method (green) and voxel method (red). The middle plot shows the distribution of angle values. The bottom plot shows the differences between the found angles.*

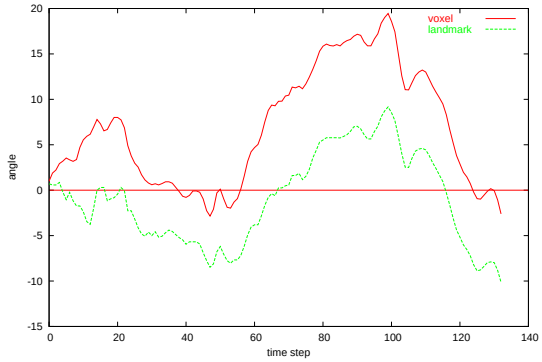

Figure 4: *Cumulated angles (top) and angle difference (bottom).*

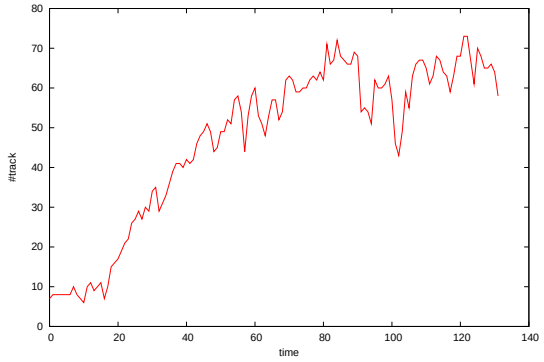

Figure 5: *Number of landmarks.*

Several relevant biological insights can be obtained from the right image in figure1. The feature tracks that different chromatin regions in the cell nucleus drift apart whilst keeping a more or less coherent shape. This insight seems support the theory that the expansion of chromatin is linear and reorganization of the cell nucleus does not occur during this phase.

Figure 4 shows a systematic rotation in one direction at a low frequency of the cell nucleus Whether this rotation is caused by forces exerted by neighboring cells or from vibrations remain a research issue.

5. Discussion

The angles found by landmark and voxel methods differ substantially at the beginning of the time series (see figure 4). An explanation for this is that the landmark method has only a few landmarks in the beginning of the time series. The differences between angles is very small when more landmarks are used. Figure 5 shows the number of landmarks used for the decondensation time series.

The angle values of the landmark based method depend on two factors. Firstly, the positions of the features computed by the feature detection and tracking algorithm will influence the landmark difference function (see equation 4). Second, the number and distribution of landmarks will influence the optimization of equation 3. A large number of uniformly distributed landmarks are preferred.

The angle values of the voxel based method depend on the numerical errors made in computation of the transformed data. This is most apparent when computing rotations in the YZ and XZ-planes, since the resolution along the Z-axis is four times less than in the XY-plane.

Timing

Table 1 shows the compute times needed for both methods. The landmark method involves three steps: feature detection, feature tracking and optimization of equation 3. The voxel method uses the acquired data directly.

	Landmark	Voxel
Detection	15 min	
Tracking	3 sec	
Optimization	20 sec	5 hour

Table 1: *Timings for the landmark and voxel methods.*

The landmark method is significantly faster in computation time. However the selection of a suitable feature definition usualy is a tedious process requiring interactive adaptation of the user[4]. If a large collection of similar sets has to be corrected this process has to be performed only once.

The time needed for the optimization step in the voxel method is linear in the number of voxels in the data. For the landmarks method the tracking and optimization steps scale with the number of landmarks.

Applicability

The landmark method depends on the availability of a sufficient number of suitable landmarks. The method can be applied only if suitable landmarks can be defined. The voxel based method doesn't rely on domain knowledge and can be applied directly to the data.

Improvements

Both methods use only two consecutive time steps in the dataset. Additional information could be gained by taking more data into account. For example, the methods could be improved by using a sequence of data sets M_t, ..., M_{t+N}, and the computed rotations and translation could be used to improve the estimation between time steps.

6. Conclusions

Filtering external motion is an essential first step for the visualization and analysis of 4D cellular data acquired from confocal microscopy. We have compared the usage of the landmark based method with the voxel based method. Landmark based methods are fast and work well if a sufficient number of landmarks can be determined. Voxel based methods are computationally more expensive, but can be applied directly to any time series and does not require additional knowledge about the data.

The methods have been applied to a time series of the decondensation process. Filtering external motion was instrumental in the formulation of many conjectures about chromatin decondensation in living cells.

References

1. J.B.A Maintz and M.A. Viergever. A survey of medical image registration. In U. Spetzger, H.S. Stiehl, and J.M. Gilsbach, editors, *Navigated Brain Surgery*, pages 117–136. Springer Verlag, 1999.

2. W. Press, B. Flannery, S. Teukolskt, and W. Vettering. *Numerical Recipes in C*. Cambridge University Press, Cambridge, 1988.

3. W.C. de Leeuw and R. van Liere. Chromatin decondensation: a case study of tracking features in confocal data. In K. Joy, A. Varshney, and T. Ertl, editors, *Proceedings IEEE Visualization 2001*, pages 441–444. IEEE Computer Society Press, 2001.

4. E.M.M. Manders, R. Hoebe, J. Strackee, A.M. Vossepoel, and J.A. Aten. The largest contour segmentation; a tool for the localization of spots in confocal images. *Cytometry*, 23:15–21, 1995.